Anal. Chem. **2003,** *75,* 5936−5943

Femtomolar Detection of Prostate-Specific Antigen: An Immunoassay Based on Surface-Enhanced Raman Scattering and Immunogold Labels

Desiree S. Grubisha, Robert J. Lipert,* Hye-Young Park, Jeremy Driskell, and Marc D. Porter*

Microanalytical Instrumentation Center, Ames Laboratory—USDOE, and Department of Chemistry, Iowa State University, Ames, Iowa 50011

A novel reagent for low-level detection in immunoadsorbent assays is described. The reagent consists of gold nanoparticles modified to integrate bioselective species (e.g., antibodies) with molecular labels for the generation of intense, biolyte-selective surface-enhanced Raman scattering (SERS) responses in immunoassays and other bioanalytical applications. The reagent is constructed by coating gold nanoparticles (30 nm) with a monolayer of an intrinsically strong Raman scatterer. These monolayer-level labels are bifunctional by design and contain disulfides for chemisorption to the nanoparticle surface and succinimides for coupling to the bioselective species. There are two important elements in this label design; it both minimizes the separation between label and particle surface and maximizes the number of labels on each particle. This approach to labeling also exploits several other advantages of SERS-based labels: narrow spectral bandwidth, resistance to photobleaching and quenching, and long-wavelength excitation of multiple labels with a single excitation source. The strengths of this strategy are demonstrated in the detection of free prostate-specific antigen (PSA) using a sandwich assay format based on monoclonal antibodies. Detection limits of ∼1 pg/mL in human serum and ∼4 pg/mL in bovine serum albumin have been achieved with a spectrometer readout time of 60 s. The extension of the method to multianalyte assays (e.g., the simultaneous determination of the many complexed forms of PSA) is discussed.

A host of different immunoassay readout techniques has been developed in past years.[1] The more established approaches include scintillation counting,[2] fluorescence,[3,4] chemiluminescence,[5] electrochemical,[6] and enzymatic methods.[1,7] Recently, strategies based on surface plasmon resonance,[8−13] surface-enhanced Raman scattering (SERS),[14−16] quantum dots,[17−22] microcantilevers,[23,24] and atomic force microscopy[25−27] have been devised. Because of its inherently high sensitivity, fluorescence-based detection is among the most used readout modality.

This paper describes our latest findings from a continuing investigation of SERS as a multiplexed, immunoassay readout concept.[16] In its traditional formats (i.e., normal and resonance),

* To whom correspondence should be addressed. E-mail: blipert@porter1.ameslab.gov.

(1) *Immunoassay*; Diamandis, E. P., Christopoulos, T. K., Eds.; Academic Press: New York, 1996.
(2) Gutcho, S.; Mansbach, L. *Clin. Chem.* **1977**, *23*, 1609−14.
(3) Vuori, J.; Rasi, S.; Takala, T.; Vaananen, K. *Clin. Chem.* **1991,** *37*, 2087−92.
(4) Xu, Y. Y.; Pettersson, K.; Blomberg, K.; Hemmila, I.; Mikola, H.; Lovgren, T. *Clin. Chem.* **1992**, *38*, 2038−43.
(5) Brown, C. R.; Higgins, K. W.; Frazer, K.; Schoelz, L. K.; Dyminski, J. W.; Marinkovich, V. A.; Miller, S. P.; Burd, J. F. *Clin. Chem.* **1985**, *31*, 1500−5.
(6) Hayes, F. J.; Halsall, H. B.; Heineman, W. R. *Anal. Chem.* **1994**, *66*, 1860−5.
(7) Butler, J. E. *J. Immunoassay* **2000**, *21*, 165−209.
(8) Lyon, L. A.; Musick, M. D.; Natan, M. J. *Anal. Chem.* **1998**, *70*, 5177−83.
(9) Knoll, W.; Zizlsperger, M.; Liebermann, T.; Arnold, S.; Badia, A.; Liley, M.; Piscevic, D.; Schmitt, F. J.; Spinke, J. *Colloids Surf., A* **2000**, *161*, 115−37.
(10) Liebermann, T.; Knoll, W.; Sluka, P.; Herrmann, R. *Colloids Surf. A* **2000**, *169*, 337−50.
(11) Nelson, B. P.; Grimsrud, T. E.; Liles, M. R.; Goodman, R. M.; Corn, R. M. *Anal. Chem.* **2001**, *73*, 1−7.
(12) Lee, H. J.; Goodrich, T. T.; Corn, R. M. *Anal. Chem.* **2001**, *73*, 5525−31.
(13) Wegner, G. J.; Lee, H. J.; Corn, R. M. *Anal. Chem.* **2002**, *74*, 5161−8.
(14) Rohr, T. E.; Cotton, T.; Fan, N.; Tarcha, P. J. *Anal. Biochem.* **1989**, *182*, 388−98.
(15) Dou, X.; Takama, T.; Yamaguchi, Y.; Yamamoto, H.; Ozaki, Y. *Anal. Chem.* **1997**, *69*, 1492−5.
(16) Ni, J.; Lipert, R. J.; Dawson, G. B.; Porter, M. D. *Anal. Chem.* **1999**, *71*, 4903−8.
(17) Chan, W. C. W.; Nie, S. *Science (Washington, D. C.)* **1998**, *281*, 2016−8.
(18) Mattoussi, H.; Mauro, J. M.; Goldman, E. R.; Anderson, G. P.; Sundar, V. C.; Mikulec, F. V.; Bawendi, M. G. *J. Am. Chem. Soc.* **2000**, *122*, 12142−50.
(19) Sun, B.; Xie, W.; Yi, G.; Chen, D.; Zhou, Y.; Cheng, J. *J. Immunol. Methods* **2001**, *249*, 85−9.
(20) Goldman, E. R.; Anderson, G. P.; Tran, P. T.; Mattoussi, H.; Charles, P. T.; Mauro, J. M. *Anal. Chem.* **2002**, *74*, 841−7.
(21) Speckman, D. M.; Jennings, T. L.; LaLumondiere, S. D.; Moss, S. C. *Mater. Res. Soc. Symp. Proc.* **2002**, *676*, Y3.6.1−6.
(22) Tran, P. T.; Goldman, E. R.; Anderson, G. P.; Mauro, J. M.; Mattoussi, H. *Proc. SPIE-Int. Soc. Opt. Eng.* **2002**, *4636*, 23−30.
(23) Wu, G.; Datar, R. H.; Hansen, K. M.; Thundat, T.; Cote, R. J.; Majumdar, A. *Nat. Biotechnol.* **2001**, *19*, 856−60.
(24) Grogan, C.; Raiteri, R.; O'Connor, G. M.; Glynn, T. J.; Cunningham, V.; Kane, M.; Charlton, M.; Leech, D. *Biosens. Bioelectron.* **2002**, *17*, 201−7.
(25) Allen, S.; Chen, X.; Davies, J.; Davies, M. C.; Dawkes, A. C.; Edwards, J. C.; Roberts, C. J.; Sefton, J.; Tendler, S. J.; Williams, P. M. *Biochemistry* **1997**, *36*, 7457−63.
(26) Jones, V. W.; Kenseth, J. R.; Porter, M. D.; Mosher, C. L.; Henderson, E. *Anal. Chem.* **1998**, *70*, 1233−41.
(27) Allen, S.; Chen, X.; Davies, J.; Davies, M. C.; Dawkes, A. C.; Edwards, J. C.; Roberts, C. J.; Tendler, S. J. B.; Williams, P. M. *Appl. Phys. A: Mater. Sci. Process.* **1998**, *A66*, S255−61.

10.1021/ac034356f CCC: $25.00
Published on Web 09/23/2003

Raman spectroscopy lacks the sensitivity required for a readout strategy. Using silver and gold nanoparticles as enhancing substrates, however, recent reports have shown that the sensitivity of SERS can rival that of fluorescence.[28−30] This breakthrough has led to renewed interest in the exploration of this information-rich spectroscopy as a tool for rapid, low-level readout.[16, 31−36]

SERS has three more characteristics that point to its potential as a multiplexed readout technique.[16,37] First, most Raman bands are 10−100 times narrower than those of fluorescence, reducing the likelihood of spectral overlap when multiple labels are used. Second, the optimum SERS excitation wavelength is dependent on the chemical/physical properties of the enhancing substrate and not the photophysics of the scatterer, facilitating multilabel readout by requiring only one excitation wavelength. Third, Raman responses are much less susceptible to photobleaching than fluorescence, enabling the use of extended signal averaging to lower detection limits.

The list of attributes can be expanded upon examining scenarios for the development of a SERS-based readout concept. Scheme 1, which idealizes our past approach for a dual-analyte sandwich immunoassay,[16] serves as a basis for identifying more subtle attributes. In Scheme 1, a set of immobilized antibodies selectively captures the target antigens, which are then detected after the directed uptake of gold nanoparticles labeled with both tracer antibodies and intrinsically strong Raman scatters (i.e., Raman reporter molecules (RRMs)). Multiple analytes can therefore be determined by immobilizing a mixture of different capture antibodies and using nanoparticles coated with different sets of RRMs and tracer antibodies.

The added advantages in this strategy reflect the use of gold colloids in label development. First, gold is a strongly enhancing surface at long-wavelength excitation. Readout is therefore less susceptible to interference by native fluorescence. Second, each nanoparticle is coated with a large number of RRMs (10^3−10^4). As such, the response of an individual binding event is markedly amplified. Third, gold surfaces are readily modified by thiols and disulfides.[38] This chemistry provides a versatile platform for label construction.

Herein, we discuss advances in our labeling and detection strategy that yield a significant improvement in detection capabilities. Our earlier procedure[16] (Scheme 2A) prepared tracer nanoparticles by the physisorption of antibodies on gold colloids that had been previously coated with a partial monolayer of RRMs based on aromatic thiols. However, the exchange of physisorbed antibodies between nanoparticles with different RRMs degraded performance. The new procedure (Scheme 2B) addresses this problem by producing particles coated with a thiolate-based monolayer that has a terminal succinimide group. This group can then react with the amines of a protein to form an amide linkage. The revised procedure also increases RRM surface concentration and employs monoclonal antibodies as biospecific elements, amplifying the response and binding affinities, respectively. This paper applies this strategy to the low-level detection of prostate-specific antigen (PSA).

Prostate cancer is the second leading cause of cancer-related deaths in adult males in the United States. PSA, a 33-kDa glycoprotein, has been used as a prostate cancer marker since

Scheme 1

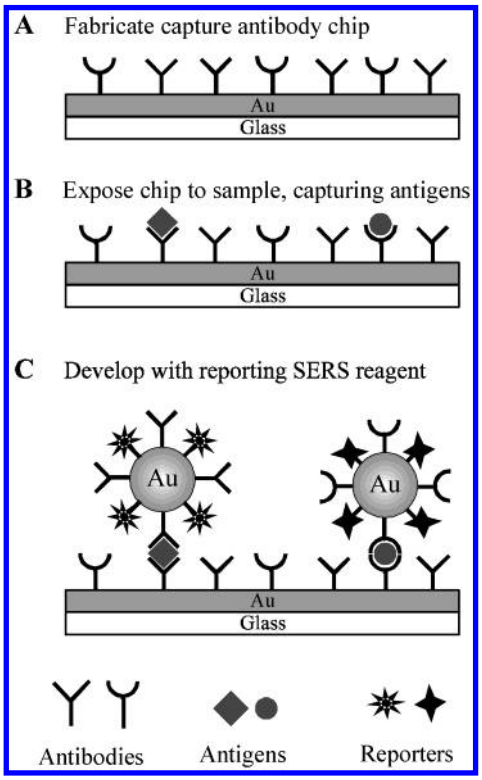

Scheme 2

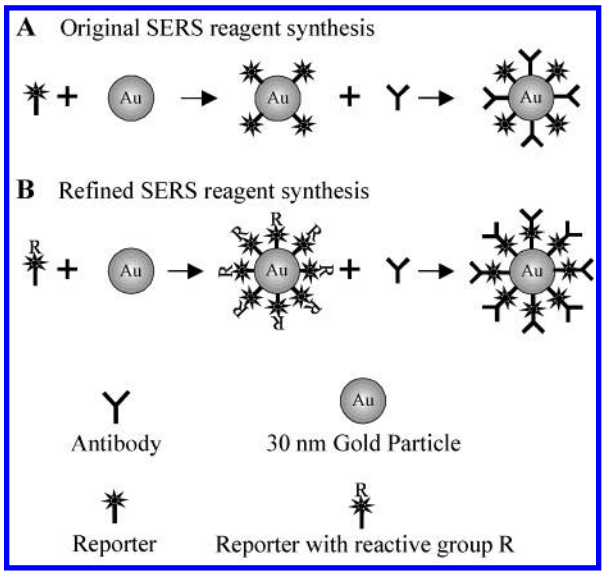

(28) Nie, S.; Emory, S. R. *Science (Washington, D. C.)* **1997**, *275*, 1102−6.
(29) Kneipp, K.; Wang, Y.; Kneipp, H.; Perelman, L. T.; Itzkan, I.; Dasari, R. R.; Feld, M. S. *Phys. Rev. Lett.* **1997**, *78*, 1667−70.
(30) Kneipp, K.; Kneipp, H.; Itzkan, I.; Dasari, R. R.; Feld, M. S. *Chem. Rev.* **1999**, *99*, 2957−75.
(31) Freeman, R. G.; Grabar, K. C.; Allison, K. J.; Bright, R. M.; Davis, J. A.; Guthrie, A. P.; Hommer, M. B.; Jackson, M. A.; Smith, P. C.; et al. *Science* **1995**, *267*, 1629−31.
(32) Keating, C. D.; Kovaleski, K. M.; Natan, M. J. *J. Phys. Chem. B* **1998**, *102*, 9404−13.
(33) Graham, D.; Mallinder, B. J.; Smith, W. E. *Biopolymers* **2000**, *57*, 85−91.
(34) Graham, D.; Mallinder, B. J.; Smith, W. E. *Angew. Chem., Int. Ed.* **2000**, *39*, 1061−3.
(35) Graham, D.; Mallinder, B. J.; Whitcombe, D.; Smith, W. E. *ChemPhysChem* **2001**, *2*, 746−8.
(36) Cao, Y. C.; Jin, R.; Mirkin, C. A. *Science* **2002**, *297*, 1536−40.
(37) Vo-Dinh, T.; Stokes, D. L.; Griffin, G. D.; Volkan, M.; Kim, U. J.; Simon, M. I. *J. Raman Spectrosc.* **1999**, *30*, 785−93.
(38) Shipway, A. N.; Katz, E.; Willner, I. *ChemPhysChem* **2000**, *1*, 18−52.

1988.[39] In blood plasma, PSA exists in both complexed and free forms, with normal levels of total PSA between 4 and 10 ng/mL.[39] The predominant form of serum PSA is a complex with α_1-antichymotrypsin, with lesser amounts bound with α_2-macroglobulin and α_1-antitrypsin.[40,41] Assays today distinguish between the different forms of PSA through unreacted epitopes in each complex. The distinction between complexed and free PSA is clinically relevant because the occurrence probability of cancer increases as the percentage of free PSA decreases.[42,43] Moreover, the reappearance of PSA after radical prostatectomy may signal cancer reemergence.[44,45] Early detection, however, is difficult because the low levels of PSA present in early stages of recurrence are below the detection capabilities of most assays.[46] There is also evidence that an ultrasensitve PSA assay may be of value in detecting breast cancer in females.[47] Hence, there is a clear need for a simple, rapid, sensitive PSA detection method.[48] We show in this paper that SERS-based readout methods can detect PSA in human serum at very low levels (~1 pg/mL). We also briefly discuss the potential application of this method to multiplexed assays.

EXPERIMENTAL SECTION

Reagents. Suspensions of unconjugated colloidal gold (32.2 ± 4.4-nm diameter, 2×10^{11} particles/mL) were purchased from Ted Pella, Inc. The matched pair of monoclonal antibodies utilized for the sandwich assay was obtained from Research Diagnostics. The pair consisted of mouse anti-human free PSA clone PSA-F65, which was used as the capture antibody after immobilization on gold-coated glass chips, and mouse anti-human PSA clone PSA-66, which was employed as the tracer antibody after conjugation to the gold particles (see below).

Serum PSA (10−30% free PSA) was purchased from Bios Pacific, and buffer packs and ImmunoPure normal human serum were acquired from Pierce Biotechnology. *N*-hydroxysuccinimide (NHS), 1,3-dicyclohexylcarbodiimide (DCCD), Tween 80, 5,5′-dithiobis(2-nitrobenzoic acid) (DNBA), and bovine serum albumin (BSA) were obtained from Aldrich. Unless otherwise specified, all reagents were used as received or were reconstituted according to standard methodologies. The preparation of dithiobis(succinimide undecanoate) (DSU) followed a modification to recent literature procedures.[49,50]

Scheme 3

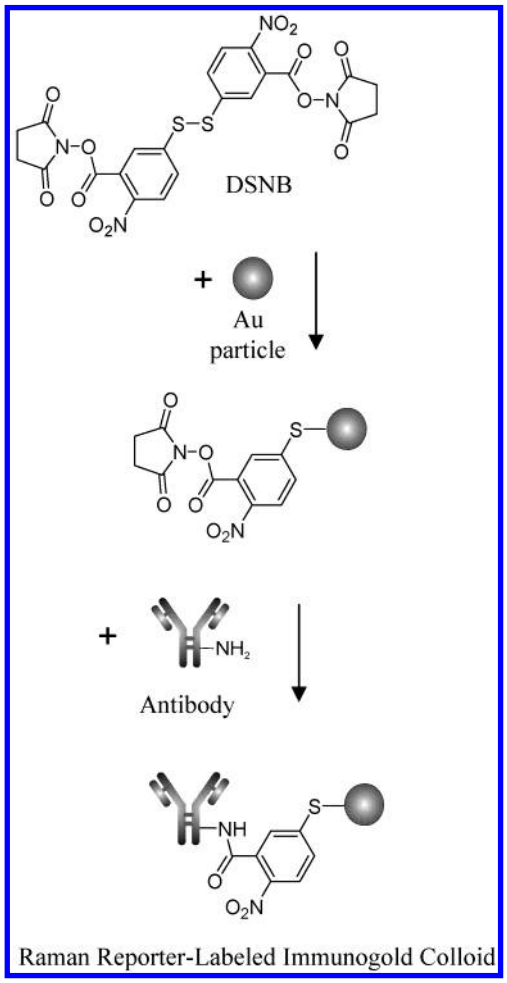

Synthesis of 5,5′-Dithiobis(succinimidyl-2-nitrobenzoate) (DSNB). To 50 mL of dry tetrahydrofuran were added 0.50 g of DNBA (1.3 mmol), 0.52 g of DCCD (2.5 mmol), and 0.29 g of NHS (2.5 mmol) in a 100-mL round-bottom flask equipped with a drying tube. The mixture was magnetically stirred at 25 °C for 12 h, filtered, and then rotoevaporated to remove solvent. The crude product was recrystallized from acetone/hexane, yielding a yellow powder: ^{1}H NMR ($CDCl_3$) δ = 8.13 (d, 2H, $^3J_{H,H}$ = 8 Hz, C_6H_4), 7.85 (d, 2H, $^3J_{H,H}$ = 8 Hz, C_6H_4), 7.97 (s, 2H, C_6H_4), 2.91 (s, 8H, CH_2).

Preparation of Raman Reporter-Labeled Immunogold Colloids. To build the new labels, we started with various derivatives of dithiobis(benzoic acid), which could easily be converted to the corresponding succinimide ester with NHS. Of those tested, DSNB is a particularly attractive example because of the strong scattering cross section of its symmetric NO_2 stretch. As such, treatment of colloidal gold with this derivative (Scheme 3) yields a coating of the thiolate of DSNB, which can couple to the primary amines of a tracer antibody by formation of an amide linkage.[49] We add that this design strategy minimizes the distance between the gold surface and label scattering center. This minimization is particularly significant because, according to a simplified electromagnetic model,[51] enhancement varies inversely

(39) Polascik, T. J.; Oesterling, J. E.; Partin, A. W. *J. Urol.* **1999**, *162*, 293−306.
(40) Stenman, U. H.; Leinonen, J.; Alfthan, H.; Rannikko, S.; Tuhkanen, K.; Alfthan, O. *Cancer Res.* **1991**, *51*, 222−6.
(41) Lilja, H.; Christensson, A.; Dahlen, U.; Matikainen, M. T.; Nilsson, O.; Pettersson, K.; Lovgren, T. *Clin. Chem.* **1991**, *37*, 1618−25.
(42) Luderer, A. A.; Chen, Y. T.; Soriano, T. F.; Kramp, W. J.; Carlson, G.; Cuny, C.; Sharp, T.; Smith, W.; Petteway, J.; Brawer, M. K. *Urology* **1995**, *46*, 187−94.
(43) Catalona, W. J.; Smith, D. S.; Wolfert, R. L.; Wang, T. J.; Rittenhouse, H. G.; Ratliff, T. L.; Nadler, R. B. *JAMA, J. Am. Med. Assoc.* **1995**, *274*, 1214−20.
(44) Ellis, W. J.; Vessella, R. L.; Noteboom, J. L.; Lange, P. H.; Wolfert, R. L.; Rittenhouse, H. G. *Urology* **1997,** *50*, 573−9.
(45) Yu, H.; Diamandis, E. P.; Wong, P. Y.; Nam, R.; Trachtenberg, J. *J. Urol.* **1997**, *157*, 913−8.
(46) Ward, A. M.; Catto, J. W. F.; Hamdy, F. C. *Ann. Clin. Biochem.* **2001**, *38*, 633−51.
(47) Melegos, D. N.; Diamandis, E. P. *Clin. Biochem.* **1996**, *29*, 193−200.
(48) Black, M. H.; Grass, C. L.; Leinonen, J.; Stenman, U. H.; Diamandis, E. P. *Clin. Chem.* **1999**, *45*, 347−54.
(49) Wagner, P.; Hegner, M.; Kernen, P.; Zaugg, F.; Semenza, G. *Biophys. J.* **1996**, *70*, 2052−66.
(50) Niemz, A.; Jeoung, E.; Boal, A. K.; Deans, R.; Rotello, V. M. *Langmuir* **2000**, *16*, 1460−2.
(51) Kneipp, K.; Kneipp, H.; Itzkan, I.; Dasari, R. R.; Feld, M. S. *J. Phys.: Condens. Matter* **2002**, *14*, R597−624.

with the 12th power of the separation distance between the scatterer and the metal particle center.

The particle workup consisted of two steps. In step 1, 100 μL of a 2.5 mM DSNB solution in acetonitrile was added to 1 mL of the unconjugated colloidal gold suspension and the mixture reacted for 3−5 h. The reporter-labeled colloids were then separated from solution by centrifugation at 10000*g* for 7 min. The clear supernatant was discarded, and the loose red sediment was resuspended in 1 mL of borate buffer (2 mM, pH 9).

In step 2, mouse anti-PSA was coupled to the gold particles via the succinimidyl terminus of the DSNB-derived coating. As such, 35 μg of detection antibody (7 μL of 5 mg/mL PSA-66 solution) was added to the 1-mL suspension of the reporter-labeled colloid. The mixture was then incubated at room temperature for 1 h. After centrifugation at 10000*g* for 7 min and removal of the supernatant, the red sediment was resuspended in 1 mL of 2 mM Tris buffer (Tris-HCl (pH 7.6), 1% BSA). We note that the use of BSA, Tween 80, or both in all of the preparative steps and in the assay protocol is part of a general procedure designed to minimize complications from nonspecific adsorption.

Preparation of Capture Antibody Substrates. Glass slides were cleaned in an ultrasonic bath under dilute surfactant solution (Micro, Cole-Parmer), deionized water, and methanol, each for 30 min. The slides were then loaded into an Edwards 306A metal evaporator and coated with 15 nm of chromium and 300 nm of gold at 0.2 nm/s at pressures less than 5×10^{-6} Torr. Next, the gold substrates were removed from the evaporator and exposed for ∼30 s to an octadecanethiol (ODT)-soaked poly(dimethylsiloxane) stamp, which had a 5-mm-diameter hole cut in its center. This step "inks" the outer portion of the gold substrate with a monolayer of ODT.[52] After inking, the substrates were rinsed with ethanol, dried under a stream of nitrogen, and immersed in a 1 mM ethanolic solution of DSU for 6−12 h. Upon removal from solution, the substrates were rinsed again with ethanol and dried under a stream of nitrogen. The result is a 5-mm-diameter domain of the succinimide ester-terminated monolayer on each substrate, surrounded by a hydrophobic ODT coating. We note that the ODT coating serves as a hydrophobic barrier that localizes aqueous protein solutions when pipetted onto the area of the substrate defined by the DSU-derived monolayer.

Anti-free PSA antibodies (PSA-65) were immobilized by pipetting 40 μL of the protein solution (100 μg/mL in 0.05 M borate buffer (pH 9) and 1% Tween 80) onto the localized domain of the DSU-modified monolayer. The reaction was allowed to progress overnight at room temperature. After rinsing three times with buffer 1 (0.01 M borate buffer (pH 9), 30 mM NaCl, 0.5% Tween 80), 40 μL of blocking buffer (5% BSA in 0.05 M borate buffer (pH 9)) was pipetted onto the surface and incubated for 1 h. The substrates were then rinsed three times with buffer 1.

Immunoassay Protocol. Free PSA dose−response curves were constructed using matrixes consisting of normal human serum, 10 mM phosphate-buffered saline (PBS, KH_2PO_4/K_2HPO_4 (pH 7.5), 150 mM NaCl, 0.1% BSA, 0.5% Tween 80, 0.02% NaN_3), and a 1:1 mixture of human serum and PBS, following the typical procedure for a sandwich-type assay. For each matrix, 40-μL aliquots of PSA solutions of various concentrations were pipetted onto a capture antibody-coated substrate and allowed to react for 3 h at room temperature. After rinsing three times with buffer 2 (10 mM PBS buffer (pH 7.5), 0.5% Tween 80, 0.02% NaN_3), the sample was exposed to 40 μL of the immunogold detection reagent for 6 h. All samples were then rinsed three times with buffer 2 and once with deionized water and dried under a stream of nitrogen before SERS characterization. We found that Tween concentrations of 0.1−0.5% in the rinse buffer were generally effective in minimizing nonspecifically bound protein, while maintaining the hydrophobic integrity of the ODT domain.

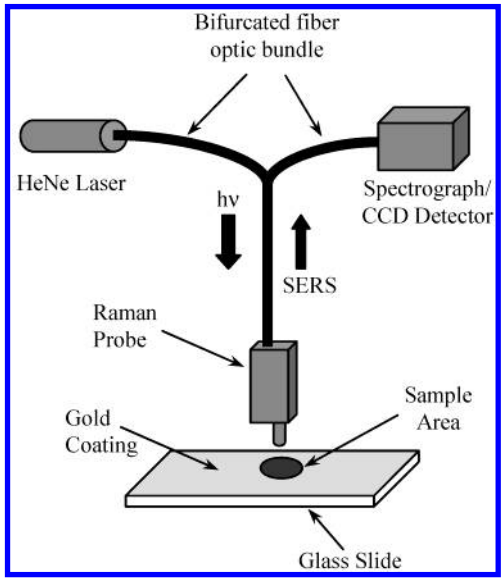

Figure 1. Experimental setup for measuring PSA levels in human serum using surface-enhanced Raman spectroscopy.

Instrumentation. (i) SERS Measurements. Figure 1 shows the spectroscopic setup. A fiber-optic-based Raman system, NanoRaman I, from NanoRaman Instruments was used for all Raman data generation. The system consists of three major subassemblies: laser light source, spectrograph, and fiber-optic probe. The light source is a 30-mW, 632.8-nm HeNe laser, while the spectrograph consists of an *f*/2.0 Czerny−Turner imaging spectrometer (6−8-cm^{-1} resolution, no moving parts) and a thermoelectrically cooled (0 °C) Kodak 0401E CCD. The fiber-optic probe (1.75 × 2.5 × 6 in) utilizes band-pass and long-pass filters for laser light (OD 6) and fiber background (OD 4) rejection. The probe objective provides a numerical aperture of 0.65 while maintaining a relatively long working distance of 3 mm. The laser spot size on the sample surface is ∼22 μm in diameter. A Windows-based Visual Basic program controls the system. All spectra were collected with a 60-s integration time. The positions of the Raman bands were determined by comparisons to the known positions of bands for solid naphthalene.[53]

(ii) Infrared Spectroscopy. Infrared reflection spectra were acquired with a Nicolet 850 FT-IR spectrometer, purged with liquid N_2 boil-off, and equipped with a liquid N_2-cooled HgCdTe detector. Spectra were obtained using *p*-polarized light incident at 80° with respect to the surface normal. The spectra were recorded as -log-(R/R_0), where R is the sample reflectance and R_0 is the reflectance of an octadecanethiolate-d_{37} monolayer-coated Au reference. The

(52) Chen, C. S.; Mrksich, M.; Huang, S.; Whitesides, G. M.; Ingber, D. E. *Biotechnol. Prog.* **1998**, *14*, 356−63.

(53) McCreery, R. L. http://chemistry.ohio-state.edu/~rmccreer/freqcorr/images/nap.html.

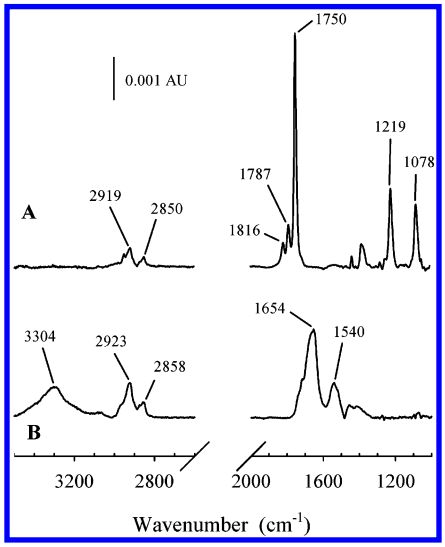

Figure 2. Infrared reflection spectra of a DSU-derived monolayer on gold before (spectrum A) and after (spectrum B) exposure to the anti-free PSA capture antibody.

spectra are an average of 512 sample and reference scans, taken at 4-cm^{-1} resolution with Happ-Genzel apodization.

(iii) X-ray Photoelectron Spectroscopy. X-ray photoelectron spectra (XPS) were acquired at room temperature with a Physical Electronics Industries 5500 multitechnique surface analysis system. This system is equipped with a hemispherical analyzer, a toroidal monochromator, a multichannel detector at 45°, and monochromatic Al Kα excitation radiation (1486.6 eV, 250 W). A pass energy of 29.35 eV was used, giving a half-width of the Au($4f_{7/2}$) peak of ~0.8 eV.

RESULTS AND DISCUSSION

Chip Characterization. The capture antibody substrate consisted of anti-free PSA bound to a gold-coated glass chip via the DSU-derived coupling agent. DSU chemisorbs to gold through cleavage of the sulfur−sulfur bond, and the formation of the resulting gold-bound thiolate and its subsequent coupling to anti-free PSA can be readily confirmed by infrared reflection spectroscopy (IRS) and XPS. The IRS results are presented in Figure 2. The three bands around 1800 cm^{-1} in the spectrum of the layer formed from DSU (Figure 2A) are assigned to the carbonyl stretches of the ester (1816 cm^{-1}) and of the succinimidyl end group (1787 (in-phase) and 1750 cm^{-1} (out-of-phase)).[54] The presence of these bands, along with the succinimidyl bands at 1219 and 1078 cm^{-1} and the methylene stretches between 3000 and 2800 cm^{-1}, verifies the formation of the DSU-based coating.

IRS was also used to confirm the covalent binding of anti-free PSA to the terminal group of the gold-bound coupling layer (Figure 2B). Since the acyl carbon of the succinimidyl ester group is strongly susceptible to nucleophilic attack, reaction with the sterically accessible amines in the protein should immobilize anti-free PSA via amide linkages. As evident in Figure 2B, treatment of the DSU-modified substrate with anti-free PSA causes a marked decrease in the magnitude of the bands for the succinimidyl group (e.g., 1750, 1219, and 1078 cm^{-1}). Moreover, three readily identifiable bands, which are located at 3304 (N−H stretch), 1654 (amide I), and 1540 cm^{-1} (amide II), have appeared. The new bands reflect the presence of amides inherent in the native antibody as well as those formed by the reaction of the succinimidyl groups of DSU with amines in the protein. Coupled with earlier reports,[26,49,55] which, in part, studied the hydrolysis rate of the succinimidyl terminal group of DSU-derived monolayer under similar conditions,[26] the differences in Figure 2 support the covalent attachment of anti-free PSA to the underlying substrate.

The XPS characterizations are in agreement with the IRS findings. The results for both modified surfaces are given in Table 1. As expected, survey spectra for the two different coatings showed only the presence of carbon, oxygen, nitrogen, and sulfur. For the DSU-based coating, the C(1s) region was composed of a lower energy band (284.4 eV), attributed to the alkyl chain structure of the coating, and a higher energy band (289.0 eV), assigned to the different types of carbonyl carbon.[56] Two bands were also observed in the O(1s) and S(2p) regions. In the O(1s) region, the band at 534.9 eV is ascribed to the oxygen of the ester linkage and that at 532.5 eV is assigned to the remaining carbonyl oxygens.[56,57] In the S(2p) region, the positions of the features in the doublet that arises from spin−orbit coupling ($2p_{3/2}$, 161.8 eV; $2p_{1/2}$, 162.9 eV) are consistent with the presence of gold-bound thiolates formed by the adsorption of thiols and disulfides on gold.[58,59] In contrast, there was only one band observed in the N(1s) region. The location of this band (401.9 eV) agrees with the presence of an electron-withdrawing group attached to nitrogen, as is the case for the succinimidyl nitrogen.[56]

After treatment with anti-free PSA, all XPS features undergo a general broadening, which limited the ability to carry out an in-depth compositional analysis. There were, however, two readily identifiable changes that support the coupling of anti-free PSA to the DSU-derived coating. First, the N(1s) band shifts from 401.9 to 400.5 eV. This shift is ascribed to the loss of the succinimidyl end group and the appearance of the numerous nitrogen functionalities in the immobilized protein.[60] Second, the intensity of the S(2p) couplet is greatly diminished. The decrease in intensity reflects the attenuation of photoelectrons by the immobilized protein.

Detection Reagent Characterization. The new RRMs, which were prepared by reacting DNBA with NHS to form the bis-(succinimide ester), yield a coating on gold that can act as a coupling agent in the same manner as the DSU-based monolayer. Figure 3 shows the IRS spectra for a monolayer of DSNB spontaneously adsorbed on gold-coated glass before and after exposure to anti-PSA. The as-formed layer has carbonyl stretches at 1812, 1789, and 1748 cm^{-1} and strong symmetric and asymmetric nitro stretches at 1343 and 1533 cm^{-1}, respectively. As with the DSU-based monolayer, the spectrum for the DSNB-derived monolayer undergoes a similar set of changes following exposure to anti-PSA. Three new bands appear (3292 (N−H stretch), 1665

(54) Frey, B. L.; Corn, R. M. *Anal. Chem.* **1996**, *68*, 3187−93.
(55) Duhachek, S. D.; Kenseth, J. R.; Casale, G. P.; Small, G. J.; Porter, M. D.; Jankowiak, R. *Anal. Chem.* **2000**, *72*, 3709−16.
(56) Delamarche, E.; Sundarababu, G.; Biebuyck, H.; Michel, B.; Gerber, C.; Sigrist, H.; Wolf, H.; Ringsdorf, H.; Xanthopoulos, N.; Mathieu, H. J. *Langmuir* **1996**, *12*, 1997−2006.
(57) Zaugg, F. G.; Spencer, N. D.; Wagner, P.; Kernen, P.; Vinckier, A.; Groscurth, P.; Semenza, G. *J. Mater. Sci.: Mater. Med.* **1999**, *10*, 255−63.
(58) Bain, C. D.; Biebuyck, H. A.; Whitesides, G. M. *Langmuir* **1989**, *5*, 723−7.
(59) Biebuyck, H. A.; Whitesides, G. M. *Langmuir* **1993**, *9*, 1766−70.
(60) Jiang, L.; Glidle, A.; Griffith, A.; McNeil, C. J.; Cooper, J. M. *Bioelectrochem. Bioenerg.* **1997**, *42*, 15−23.

Table 1. Binding Energies (eV) and Compositional Assignments for XPS Spectra of DSU and DSNB Monolayers on Gold before and after Antibody Derivitization

core level	DSU/Au	anti-free PSA/DSU/Au	DSNB/Au	anti-PSA/DSNB/Au
Au($4f_{7/2}$)	83.9	83.9	83.9	83.9
S($2p_{3/2}$)	161.8	161.8	162.2	162.2
S($2p_{1/2}$)	162.9	162.9	nd[a]	nd
C(1s)	289.0	288.5	288.4	288.1
C(1s)	284.4	284.9, 286.4 (sh)	284.6	284.8, 285.9 (sh)
N(1s)	401.9	400.5	405.6, 401.2	405.2, 400.0
O(1s)	532.5, 534.9	532.1	532.2	532.2

[a] nd, not detected.

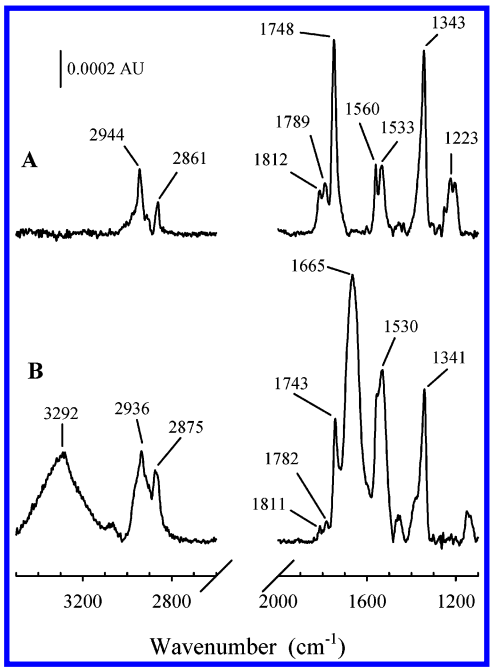

Figure 3. Infrared reflection spectra of a DSNB-derived monolayer on gold before (spectrum A) and after (spectrum B) exposure to the anti-PSA tracer antibody.

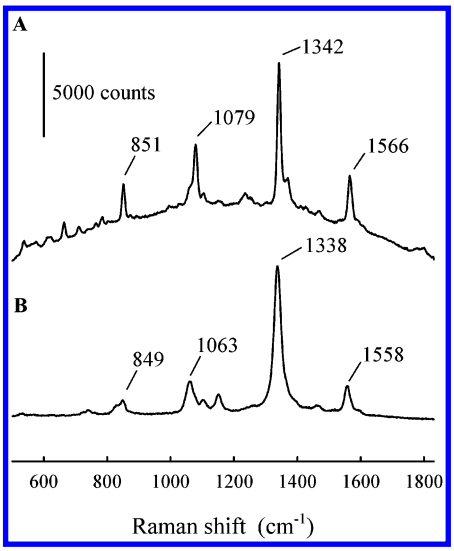

Figure 4. Raman spectra of the reporter compound: (A) Spectrum of DSNB powder; (B) SERS spectrum of gold nanoparticles following reaction with DSNB.

(amide I), and 1530 cm^{-1} (amide II)), and the three carbonyl stretches exhibit a notable decrease. The detection of residual succinimide groups is expected because the presence of an immobilized antibody will sterically hinder protein binding to neighboring succinimide moieties. Thus, BSA was used in the immunogold reagent preparation procedure to react with any exposed residual succinimide groups in order to preclude their participation in nonspecific binding.

The XPS characterizations (Table 1) also strongly mimic those for the DSU-based layer. In this case, however, there are two N(1s) bands for each sample. For the as-formed layer, bands at 401.2 and 405.5 eV are indicative of the succinimidyl nitrogen and nitro nitrogen on the aromatic ring, respectively. After exposure to anti-PSA, the band at 401.2 eV disappears and one at 400.0 eV appears. This change again parallels that for the DSU-derived coating.

SERS of Reporter-Labeled Immunogold Reagent. Raman spectra for the RRM DSNB are shown in Figure 4 before and after coupling to the gold nanoparticles. The nanoparticle sample was prepared by drop casting a small amount of the labeled colloid solution onto a gold-coated glass slide and evaporating the water-based solvent. The powder spectrum (Figure 4A) is dominated by the symmetric nitro stretch at 1342 cm^{-1}, and we attribute the band at 851 cm^{-1} to the nitro scissoring vibration. The band at 1566 cm^{-1} is assigned to an aromatic ring mode (8a),[61] and the large band at 1079 cm^{-1} is probably a succinimidyl N−C−O stretch overlapping with aromatic ring modes.

Many of the bands in the powder spectrum are present in the spectrum after DSNB is chemisorbed onto the gold nanoparticles (Figure 4B), though some have undergone a small change in position. For example, the symmetric nitro stretch has shifted from 1342 to 1338 cm^{-1}, and the 8a mode has moved from 1566 to 1558 cm^{-1}. These shifts are indicative of interactions between neighboring adsorbates and between the adsorbates and the gold surface. Additionally, since there was no detectable Raman signal for the monolayer formed from DSNB adsorbed to a smooth gold surface, the spectrum in Figure 4B illustrates that the immobilization of DSNB on the gold nanoparticles results in a significant level of enhancement, the magnitude of which will be examined in detail in future studies. Together, these results confirm that the particles have been effectively modified with the DSNB-based RRMs.

SERS Immunoassay Detection of Free PSA. The results of our SERS-based determinations for free PSA in normal human serum are shown in Figure 5. Test solutions were made by serial dilution in human serum of a 1 mg/mL PSA standard to cover the range from 1 μg/mL (30 nM) to 1 pg/mL (30 fM). The spectra

(61) Varsanyi, G. *Assignments for Vibrational Spectra of Seven Hundred Benzene Derivatives*; John Wiley & Sons: New York, 1974.

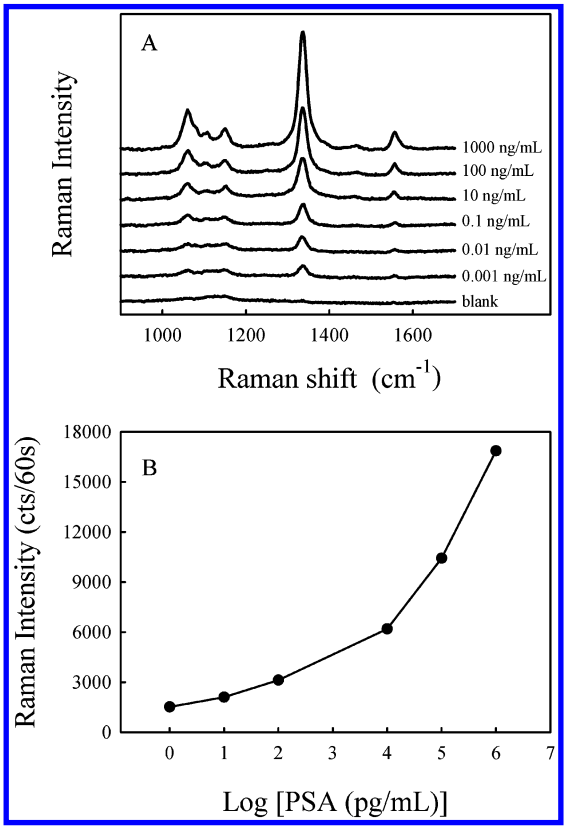

Figure 5. Demonstration of a SERS-based free PSA immunoassay. (A) SERS spectra, offset for clarity, acquired at various PSA concentrations. (B) Dose−response curve for free PSA in human serum. The dose−response curve was constructed by calculating the average reading of the response for 6−8 different locations on the surface of each sample, which typically varied by 10% (see text for further details).

in Figure 5A were obtained using 60-s integrations after completion of the immunoassay protocol outlined above. As is evident, the features diagnostic of the DSNB-labeled nanoparticles exhibit a strong increase as the PSA level increases. These changes span more than 6 orders of magnitude, thus encompassing concentration levels critical to prostate cancer diagnosis.[39]

The lower limit of detection is defined by the nonspecific adsorption of the labeled nanoparticles, as demonstrated by the signal observed for the blank serum sample. Blanks prepared without BSA and Tween 80 as additives yielded signals that were several times larger than those obtained with the use of additives. In contrast, the packing constraints imposed by the labeled particle size should control the upper limit of the dynamic range. Though only examined in a preliminary manner, tests place the upper limit at ~10 μg/mL.

A more detailed treatment of our findings is presented by the dose−response curve in Figure 5B. This curve was constructed by plotting the scattering intensity of the symmetric nitro stretch (1338 cm^{-1}, full width at half-maximum of 22 cm^{-1}). Each data point represents the average of six to eight readings across the sample surface. Variations in signal strength across the surface of each chip were typically ~10%. However, signal strengths up to twice as large as those represented in the plot were observed ~20% of the time. The dose−response curve was constructed by omitting the data for these "hot spots". These hot spots could possibly reflect the presence of domains where there are higher localized concentrations of binding sites and, therefore, higher particle concentrations. Images of the surface using atomic force microscopy (AFM), however, argue that particle densities are reasonably homogeneous over areas irradiated by the laser source. On the other hand, AFM imaging revealed a small number of particle aggregates that could account for the hot spots. A third possibility arises from the existence of "hot particles". Recent studies have shown that enhancement factors are strongly dependent on particle size, shape, and excitation wavelength and that a small fraction of particles exhibit markedly larger enhancements.[28,29] We are currently designing experiments to better understand the origin of the hot spots and potentially utilize them in future assays.

The dose−response curve shows that our detection platform can determine free PSA at very low concentrations in human serum. The detection limit is ~1 pg/mL.[62] These results compare favorably with commercial assays based on radiometric, chemiluminescent, and ELISA methods, which have detection limits ranging from 3 to 1000 pg/mL free PSA.[46] Additional studies were performed in which PSA was added to 10 mM PBS that contained 0.1% BSA and 0.5% Tween 80. These studies yielded a detection limit of 4 pg/mL free PSA, based on a concentration that produces a signal three times the standard deviation of the background. Similar results were obtained in an analyte matrix of a 1:1 mixture of PBS/serum. Thus, the assay appears applicable to a range of sample matrixes.

The ability to detect exceedingly small amounts of analyte using our monoclonal-based assay format is underscored by a rough estimate of the number of molecular recognition events responsible for the response at the limit of detection. At a detection limit of 4 pg/mL, a 40-μL solution of free PSA contains 160 fg (~3×10^6 molecules) of free PSA. If we assume that (1) the capture surface exhaustively binds all of the proteins, (2) the captured antigens are uniformly distributed across the 5-mm-diameter surface of the capture substrate, and (3) the binding stoichiometry between the nanoparticles and captured antigen is 1:1, then there are only ~60 PSA molecules in the 22-μm-diameter area irradiated by the laser source. This analysis shows that the combination of surface enhancement with respect to the close proximity of the scattering site to the particle surface, the amplification due to the large number of RRMs coating each particle (preliminary estimates indicate that there are ~10^3 RRMs tethered to each nanoparticle), and the binding affinity of monoclonal antibodies leads to an extremely low level of detection.[63]

Based on the estimate of the number of recognition events detected in our PSA assay, projections can be made which strongly

(62) Recall that the capture antibody was anti-free PSA while the antigen was serum PSA containing only 10−30% free PSA. The projected detection limit estimates are, however, based on the total PSA concentration of the antigen standard and therefore the detection limits for free PSA should be somewhat lower.

(63) Our past work[16] reported a limit of detection of ~30 ng/mL for an assay using polyclonal antibodies. The ~30000× improvement described herein reflects a combination of several factors. These factors include a doubling in the label surface concentration on each particle, a larger Raman scattering cross section for the new label (~5×), and the use of monoclonal vs polyclonal antibodies (~1000× higher affinity). We have also employed a different Raman spectrometer. This instrument uses a slightly shorter excitation wavelength for greater enhancement and has an improved collection efficiency (>4× improvement in signal-to-noise ratio). While only rough estimates, it is the combination of these improvements that lead to the markedly lower limit of detection in our PSA assay.

argue that the technique can be extended to single-molecule detection. There are two clear avenues to reach such a level. The first avenue uses labels that undergo both resonance and surface enhancement. With resonance enhancement, intensities can be 2−6 orders of magnitude greater than those based on normal Raman scattering.[64] The second avenue takes advantage of recent reports that have shown that the surface enhancement for slightly larger gold particles (e.g., 60 nm for our excitation wavelength) is greater than that for 30-nm particles.[65] Taken together, the ability to detect the binding of a single antigen appears to be well within reach and should be of immense value in the ultra-low-level detection of a wide range of biomarkers used in early disease diagnosis and other assay applications. Low-level detection becomes even more important as the degree of multiplexing increases, e.g., in instances where screening for multiple analytes at a single address is of interest.

CONCLUSIONS

This report has shown that an important biomarker for early cancer diagnosis can be detected in serum samples at very low concentrations by a SERS-based readout method. This strategy is potentially capable of encompassing a wide range of applications, especially in view of the opportunities to multiplex through the judicious design of more labeled nanoparticles. As such, multiple analytes could be concurrently identified by the position of a characteristic feature of the Raman label and then quantified by its intensity. Assays could therefore be developed for the high-sensitivity, simultaneous screening of a battery of cancer markers using a single serum sample, saving time, reducing assay costs, and potentially leading to earlier diagnosis. Experiments are underway to test this concept by developing an assay for the concurrent determination of free and total PSA, a ratio shown to improve the reliability of prostate cancer diagnosis with respect to those that rely on interpretations from the levels for one marker.[42,43]

(64) Morris, M. D.; Wallan, D. J. *Anal. Chem.* **1979**, *51*, 182A−3A, 185A6A, 188A, 190A, 192A.
(65) Krug, J. T., II.; Wang, G. D.; Emory, S. R.; Nie, S. *J. Am. Chem. Soc.* **1999**, *121*, 9208−9214.

ACKNOWLEDGMENT

This work was supported by Concurrent Analytical, Inc., through a grant from the DARPA CEROS program and by the Microanalytical Instrumentation Center of Iowa State University. The Ames Laboratory is operated for the U.S. Department of Energy by Iowa State University under contract W-7405-eng-82.

Received for review April 7, 2003. Accepted August 25, 2003.

AC034356F